JURNAL ILMU KEFARMASIAN INDONESIA
Indonesian Journal of Pharmaceutical Sciences
ISSN p-ISSN 1693-1831 (Print) e-ISSN 2614-6495 (Online) PUBLISHER : Faculty of Pharmacy Universitas Pancasila

Bioactive compounds of *Plukenetia volubilis* L. as c-Met tyrosine kinase ınhibitors for gastric anticancer: in silico study

Silma Lutfi Farwah[1], Saeful Amin[1*], Ade Yeni Aprillia[1]

[1]*Department of Pharmacy, Faculty of Pharmacy, University of Bakti Tunas Husada, Tasikmalaya, 46115, Indonesia.*

*Corresponding Author: saefulamin@universitas-bth.ac.id

Received: 20 June 2026 / Accepted: 30 August 2026

ABSTRACT: Gastric cancer remains one of the most aggressive malignancies worldwide due to its high incidence and mortality rates. Although tyrosine kinase inhibitors have demonstrated therapeutic efficacy, their use is often associated with adverse effects, highlighting the need for safer anticancer agents. *Plukenetia volubilis* L. is known to be rich in bioactive compounds, particularly fatty acids and phenolic compounds with natural antioxidant activity. Accordingly, this study aimed to evaluate the potential of *Plukenetia volubilis* L. compounds as gastric anticancer candidates through inhibition of the c-Met tyrosine kinase receptor (PDB ID: 3DKC) using an integrated in silico approach. To this end, screening drug-likeness using swissADME, molecular docking using the PyRx algorithm, molecular dynamics simulation using AMBER 22, and ADMET prediction were performed using pkCSM. Among the 28 identified compounds, ten met the drug-likeness criteria for oral drug candidates. Redocking validation using adenosine-5′-triphosphate produced a root mean square deviation value of 1.31 Å, indicating a reliable docking method. Molecular docking results show that apigenin, pinoresinol, mycophenolic acid, and oleuropein aglycone exhibit the strongest binding affinities toward c-Met tyrosine kinase, with binding free energies of −7.77, −7.57, −7.24, and −6.90 (kcal/mol), respectively. Further analysis demonstrates that apigenin forms the most stable ligand–receptor complex during molecular dynamics simulation and possesses favorable pharmacokinetic properties with no predicted hepatotoxicity based on absorption, distribution, metabolism, excretion, and toxicity analysis. In conclusion, apigenin emerges as the most promising gastric anticancer candidate from *Plukenetia volubilis* L. through c-Met tyrosine kinase inhibition and warrants further experimental validation.

KEYWORDS: Apigenin, c-Met tyrosine kinase, gastric cancer, molecular dynamic, *Plukenetia volubilis* L.

INTRODUCTION

Cancer is a disease characterized by uncontrolled cell growth and proliferation resulting from genetic and molecular changes, enabling it to form tumors, invade surrounding tissues, and metastasize to other organs [1]. Gastric cancer is a type of cancer characterized by high malignancy and mortality rates. It develops in the lining of the stomach wall and is often diagnosed only at an advanced stage, resulting in limited treatment options and a poor prognosis for patients [2]. Risk factors for gastric cancer include Helicobacter pylori infection, a high-salt diet, tobacco use, and social and demographic factors. [3].

Gastric cancer remains a significant global health issue [4]. Data from the International Agency for Research on Cancer (IARC) indicate that gastric cancer is among the cancers with high global incidence and mortality rates, with more than 1,033,701 new cases and 782,685 deaths reported across 48 countries in 2018 [5]. The substantial burden of this disease underscores the need to develop more effective prevention and therapeutic strategies. Gastric cancer management encompasses surgery, chemotherapy, immunotherapy, and targeted therapy. A key molecular target is the mesenchymal-epithelial transition factor (c-MET), a receptor tyrosine kinase that regulates cell proliferation, migration, invasion, angiogenesis, and survival. c-MET activation is primarily triggered by hepatocyte growth factor (HGF), which subsequently activates various signaling pathways that drive cancer progression and metastasis. Aberrant c-MET activation has been linked to disease progression and poor prognosis in various cancers, including gastric cancer.

Inhibition c-MET activity is a strategy in cancer therapy development. Several tyrosine kinase inhibitors targeting the MET pathway such as bozitinib, savolitinib, tepotinib, capmatinib, and crizotinib have been

How to cite this article: Farwah SL, Amin S, Indriani O, Aprillia AY. Bioactive compounds of Plukenetia volubilis L. as c-Met tyrosine kinase ınhibitors for gastric anticancer: in silico study. Jurnal Ilmu Kefarmasian Indonesia. 2026. 24(2): 422-437.

https://doi.org/10.35814/jifi.v24i2.2152
ISSN: 2614-6495

developed and demonstrated therapeutic activity in cancers involving this pathway [6]. However, targeted therapies still face various limitations, including side effects, the emergence of resistance, inconsistent responses, and relatively high treatment costs. These challenges have driven the search for new inhibitor candidates with the potential for greater efficacy and improved safety profiles. Natural products represent a compelling source for developing anticancer candidates due to their structural diversity and wide range of biological activities [7].

Plukenetia volubilis L. is a plant with potential as a source of anticancer compounds. It contains various metabolites, including fatty acids, phenolic compounds, flavonoids, lignans, terpenoids, amino acids, and other organic metabolites. Compounds reported to be present in *P. volubilis* include hydroxytyrosol, bergenin, pinoresinol, apigenin, oleuropein aglycone, limonene, and aristolene [8]. These metabolites are known to exhibit various biological activities such as antioxidant, anti-inflammatory, and anticancer effects that potentially influence cancer cell proliferation and survival [9]. Unsaturated fatty acid content, particularly α-linolenic acid and linoleic acid, also contributes to the biological activity of *P. volubilis*. Furthermore, in vitro studies indicate that *P. volubilis* extracts or components can inhibit the viability and proliferation of cancer cells, including gastric cancer cells [10].

Although various studies have demonstrated the biological potential of *P.volubilis*, most research has focused on the general activity of its extracts, oils, or fractions. Information regarding the ability of its secondary metabolites to interact specifically with gastric cancer molecular targets particularly the c-MET tyrosine kinase domain remains limited. Furthermore, anticancer activity observed in in vitro assays has not yet directly elucidated the patterns of molecular interaction or the stability of the compounds in relation to the target protein. These circumstances highlight the need to identify *P.volubilis* compounds capable of inhibiting c-MET and to understand the characteristics of their interactions at the molecular level.

In silico approach can serve as an initial step to evaluate the potential of compounds prior to experimental testing. Molecular docking enables the prediction of binding affinity and interaction patterns between a compound and its target protein, while molecular dynamics simulations are used to assess the stability of the protein-ligand complex under dynamic conditions. These approaches can be complemented by analyses of drug-likeness, physicochemical properties, and pharmacokinetics to obtain a preliminary overview of the compound's suitability as a drug candidate [11].

The MET tyrosine kinase domain structure (PDB ID: 3DKC) features an ATP-binding pocket within its catalytic domain that plays a crucial role in kinase activity. Binding of a compound to this pocket has the potential to inhibit MET activity by competing with ATP. Therefore, this study aims to evaluate the potential of *P. volubilis* secondary metabolites as gastric anticancer candidates targeting the c-MET tyrosine kinase domain (PDB ID: 3DKC) using approaches involving drug-likeness assessment, molecular docking, molecular dynamics simulations, and analysis of physicochemical and pharmacokinetic properties. The study results are expected to identify potential c-MET inhibitor compounds and serve as a basis for further experimental research.

▪ MATERIALS AND METHODS

Materials

This study was conducted in silico using various software tools and databases, including MarvinSketch, AutoDockTools, Molegro Molecular Viewer, Discovery Studio Visualizer, PyRx, SwissADME, pkCSM, PubChem, the Protein Data Bank (PDB), and PDBsum. Meanwhile, molecular dynamics simulations were performed using AMBER software on the Linux operating system. The study materials consisted of 28 secondary metabolites of *Plukenetia volubilis* L., selected from 81 compounds identified in the literature based on relevant biological activities, namely antioxidant, anti-inflammatory, and anticancer properties. The target protein used was the c-MET tyrosine kinase receptor (PDB ID: 3DKC), with adenosine-5′-triphosphate (ATP) as the natural ligand and bozutinib as the comparator drug.

Receptor Analysis

The MET tyrosine kinase receptor, with PDB code 3DKC, serves as the molecular target. The quality of the receptor structure was evaluated based on crystal resolution, Ramachandran plots, LigPlot, Verify3D, and

ERRAT. This evaluation aims to ensure the suitability of the protein structure before it is used in molecular docking and molecular dynamics simulations [12].

Receptor Preparation

The structure of the c-MET tyrosine kinase receptor (PDB ID: 3DKC) was downloaded from the Protein Data Bank (PDB) in .pdb format. The receptor was prepared using AutoDockTools and Molegro Molecular Viewer by removing water molecules, isolating the native ligand, adding polar hydrogen atoms, and assigning Kollman charges. The prepared receptor structure was then saved in (.pdbqt) format for use in the molecular docking process [13].

Screening drug-likeness

Screening drug-likeness was performed using SwissADME to evaluate the physicochemical properties of the selected compounds according to Lipinski's Rule of Five. The evaluated parameters included molecular weight, lipophilicity (LogP), hydrogen bond donors, hydrogen bond acceptors, and molar refractivity. Compounds meeting the drug-likeness criteria were selected for further molecular docking analysis [14].

Ligand Preparation

The test compound ligands downloaded from the PubChem website were saved in 2D (sdf) format and converted to mol2 format. Next, the ligands were prepared in two steps. First, the ligands in 2D format were protonated at physiological pH 7.4. Then, they were saved in (.m.r.v) format. The ligand's energy was minimized by determining its conformations using the MMFF94 (Merk Molecular Force Field) parameters developed by Thomas A. Halgren (1999), which are designed to accurately represent the energy of organic molecules through a molecular mechanics approach. Ten conformations were generated to explore the various possible three-dimensional shapes of the ligand before to molecular docking. Utilization multiple conformations provides a broader overview of the potential shapes the ligand can adopt. The conformation with the lowest energy was selected as the most energetically stable one and subsequently saved in PDB (.pdb) format for molecular docking analysis [15]. Both processes were performed using MarvinSketch software version 5.2.5.1 [16].

Molecular Docking Validation (Redocking)

The molecular docking method was validated by redocking the natural ligand ATP into the active site of the c-MET receptor (PDB ID: 3DKC). The search space (grid box) was defined based on the position of the natural ligand in the ATP-binding pocket with center coordinates x = 18.294; y = 31.342; and z = 20.529 and a grid size of 50 × 50 × 50 Å. The redocking process was performed using the Lamarckian Genetic Algorithm (LGA) with a parameter of 100 GA Runs, indicating that the ligand conformation search was performed 100 times independently to obtain the most optimal and reproducible binding pose. The validity of the method was evaluated based on the Root Mean Square Deviation (RMSD) value between the redocking pose and the crystal conformation of the natural ligand. The method was considered valid if it produced an RMSD value ≤ 2.0 Å [17].

Molecular Docking and Interaction Visualization

Molecular docking was performed Molecular docking was performed using PyRx with AutoDock Vina as the docking engine to evaluate the binding affinity and interactions of compounds meeting drug-likeness criteria with the c-MET receptor (PDB ID: 3DKC). The docking process was conducted at the ATP-binding pocket using the same grid box parameters applied during docking validation. The best docking pose was selected based on the lowest predicted binding affinity and its compatibility with interactions formed with amino acid residues within the receptor's active site.

The docking results were then visualized using Discovery Studio Visualizer to analyze ligand-receptor interactions, including hydrogen bonds, hydrophobic interactions, and amino acid residues involved in complex formation. Compounds with the best binding affinity were subsequently selected for molecular dynamics analysis [18].

Molecular Dynamics Simulation

The compounds with the best molecular docking results were further analyzed using molecular dynamics simulations in AMBER 22 software running on a Linux operating system. The protein-ligand complexes were

prepared by adding hydrogen atoms, parameterizing the protein using the ff14SB force field, and parameterizing the ligand using the Antechamber and General Amber Force Field (GAFF). The system was then solvated using an explicit water model and neutralized by adding counterions using tleap. The simulations included energy minimization, gradual heating up to 320 K to achieve stable thermal conditions of the system prior to production simulations, equilibration, and production simulations for 100 ns with a 2 fs time step using the SHAKE algorithm. Complex stability was evaluated based on Root Mean Square Deviation (RMSD) and Root Mean Square Fluctuation (RMSF) values, while binding free energy was calculated using the MMGBSA and MMPBSA methods [19].

Pharmacokinetic Analysis

The pharmacokinetic analysis to be conducted will cover the absorption, distribution, metabolism, excretion, and toxicity of compounds found in the *P.volubilis*. Toxicity testing was performed on ligand compounds using pkCSM, accessed via the website (https://biosig.lab.uq.edu.au/pkcsm/). Using the SMILES codes for each tested compound on the pkCSM website, the analyzed parameters included CaCo2 (log cm/s), intestinal absorption (human) (%), Vds (Volume of distribution) in humans (log L/kg), BBB (Blood-Brain Barrier) permeability, metabolism regarding inhibition of CYP2D6 and CYP3A4, excretion via total clearance (log m1/min/kg), as well as toxicity parameters such as hepatotoxicity [20].

▪ RESULTS

Receptor Analysis

The tyrosine kinase receptor with PDB code 3DKC, as the target, represents the MET kinase domain involved in the activation of the c-Met signal transduction pathway. Before the docking process was performed, the quality of the receptor needed to be verified using parameters such as receptor resolution, the Ramachandran plot, LigPlot, Verify 3D, and ERRAT. Analysis of the crystal structure of the receptor with PDB code 3DKC shows that the 3DKC protein structure has a good resolution of 1.52 Å. The Ramachandran plot results show that 90.9% of residues are in the most favored region and 0.0% in the disallowed region , indicating that the protein structure is stable. LigPlot analysis revealed ATP interactions with key residues at the binding site [13], serving as a reference for ligand-receptor interactions accessed from https://saves.mbi.ucla.edu/. According to the International Tables for Crystallography (2012), Verify3D evaluates the compatibility between a protein's amino acid sequence and its three-dimensional structural environment, followed by ERRAT, which assesses the quality of the protein structure based on non-bonded atom–atom interactions. Although the Verify 3D score to 3DKC of 79.17% is slightly below the standard, the ERRAT result of 95.7% indicates very good structural quality. Therefore, the 3DKC protein structure is suitable for molecular docking and molecular dynamics analysis. Consequently, this target receptor proceeds to the receptor preparation stage, which aims to prepare the binding site to be available for test ligands and improve the accuracy of ligand-receptor interaction predictions in molecular docking. Figure 1 shows two of the five receptor analysis results based on Ramachandran plot parameters as an index of receptor suitability and LigPlot analysis as a reference for the interactions of the natural ligand complex with amino acids [21].

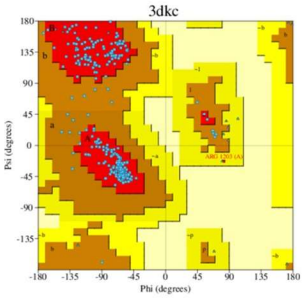

Ramachandran Plot statistics

		No. of residues	%-tage
Most favoured regions	[A,B,L]	250	90.9%
Additional allowed regions	[a,b,l,p]	24	8.7%
Generously allowed regions	[~a,~b,~l,~p]	1	0.4%
Disallowed regions	[XX]	0	0.0%
Non-glycine and non-proline residues		275	100.0%
End-residues (excl. Gly and Pro)		1	
Glycine residues		21	
Proline residues		15	
Total number of residues		312	

(a)

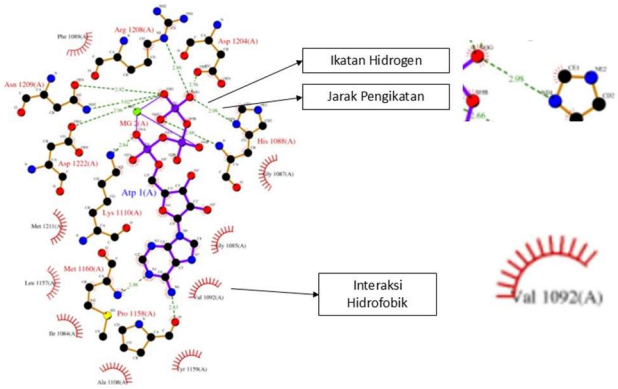

(b)

Figure 1. Two main parameters of receptor analysis. *(a)* Ramachandran plot analysis. *(b)* LigPlot visualization of the interaction between the native ligand (ATP) and the tyrosine kinase receptor (PDB code: 3DKC).

Analysis using Ramachandran plots and LigPlot indicates that the c-MET receptor (PDB ID: 3DKC) has good structural quality and a well-defined active site. Based on these results, the receptor was further prepared by removing water molecules, separating the natural ligand, adding polar hydrogen atoms, and preparing it for use in molecular docking.

Screening drug-likeness

Drug-likeness screening using SwissADME revealed that, out of 28 *P. volubilis* compounds, 10 met all of Lipinski's criteria: palmitoleic acid, myristic acid, hydroxytyrosol, pinoresinol, apigenin, mycophenolic acid, oleuropein aglycone, nagilactone, limonene, and aristolene. Compliance with parameters regarding molecular weight, lipophilicity, hydrogen bond donors and acceptors, and molar refractivity indicates that these compounds possess physicochemical properties suitable for oral drug candidates. The compounds that passed the screening are predicted to exhibit a favorable hydrophilic-lipophilic balance, suggesting potential for efficient absorption and the ability to permeate biological membranes. Based on the drug-likeness screening results presented in Table 1, 10 of the 28 tested compounds met the criteria to serve as ligand candidates [14].

Table 1. Results of drug-likeness analysis.

No	Compounds	BM (< 500 g/mol)	Lipophilicity (Log P < 5)	Hydrogen Bond Donors (< 5)	Hydrogen Bond Acceptors (< 10)	Molar Refractivity (40-130)
1.	Alpha-linolenic acid	278.43	5.66	1	2	88.99
2.	Linoleic acid	294.47	5.97	0	2	93.78
3.	L-serine	105.09	-1.97	3	4	22.18
4.	Gamma-linolenic acid	278.43	5.66	1	2	88.99
5.	Eicosatrienoic acid	306.48	5.96	1	2	98.60
6.	**Palmitoleic acid***	**253.40**	**4.67**	**0**	**2**	**78.38**
7.	Oleic acid	282.46	5.65	1	2	89.94
8.	Gondoic acid	310.51	6.41	1	2	99.55
9.	Nervonic acid	366.62	7.86	1	2	118.78
10.	Butyric acid	88.11	0.68	1	2	23.11
11.	**Myristic acid***	**228.37**	**4.45**	**1**	**2**	**71.18**
12.	Margaric acid	270.45	5.57	1	2	85.60
13.	Arachidic acid	312.53	6.62	1	2	100.03
14.	**Hydroxytyrosol***	**154.16**	**0.56**	**3**	**3**	**41.42**
15.	Bergenin	328.27	-0.80	5	9	72.80
16.	**Pinoresinol***	**358.39**	**2.26**	**2**	**6**	**94.90**
17.	**Apigenin***	**270.24**	**2.11**	**3**	**5**	**73.99**
18.	**Mycophenolic acid***	**320.34**	**2.72**	**2**	**6**	**84.35**
19.	**Oleuropein aglycone***	**378.37**	**1.57**	**3**	**8**	**94.89**
20.	**Nagilactone***	**362.37**	**1.07**	**2**	**7**	**88.61**
21.	**Limonene***	**136.23**	**3.37**	**0**	**0**	**47.12**

22. Aristolein*	**204.35**	**4.37**	**0**	**0**	**66.88**
23. L-aspartic acid	133.10	-2.04	3	5	27.59
24. 4-Aminobutanoic acid	103.12	-0.72	2	3	25.82
25. L-5-oxoproline	129.11	-0.46	2	3	32.72
26. 2-Hydroxyglutaric acid	148.11	-0.68	3	5	30.85
27. 2-Butenedioic acid	116.07	-0.35	2	4	24.41
28. L-leucine	131.17	-0.38	2	3	35.44

Note: (*) has the same bioavailability as the oral drug.

Redocking

The validation of molecular docking aims to ensure that the docking method can accurately predict ligand–receptor interactions. This process is performed through redocking of the native ligand, with a success criterion of RMSD ≤ 2 Å. A low RMSD value indicates a high similarity between the docking pose and the native ligand's crystal structure, thereby validating the method's reliability. Validation is further supported by the consistency of interaction patterns and ligand binding energies.

Result of validation yield RMSD value of 1.31 Å and a binding affinity of −7 kcal/mol. An RMSD value of ≤ 2 Å indicates that the ligand position obtained from redocking closely resembles the position of the native ligand in the crystal structure. Figure 2 shows that the docking method used is valid and suitable for analyzing the interactions of the test compound with the target receptor with PDB code 3DKC.

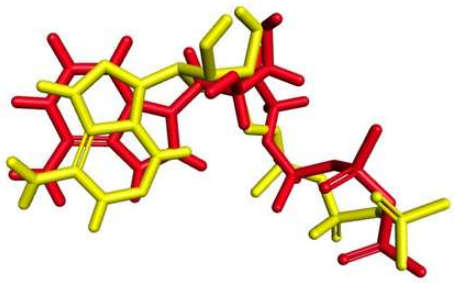

Figure 2. Overlay of the natural ligand (ATP) before redocking (red) and after redocking (yellow).

The previous figure showing the overlap between the redocked ligand and the crystal ligand reveals nearly identical positions at the binding site, indicating the success of the redocking in reproducing the original binding pose as an initial validation prior to further interaction analysis. In Figure 3, the 3D and 2D visualizations of the redocking results demonstrate the consistency of ligand interactions at the receptor's active site. In the 3D view, the ligand (ATP as a control) is stably bound to the c-MET active pocket with an orientation close to its crystal structure, indicating the positional accuracy of the docking results. Meanwhile, the 2D LigPlot analysis clarifies the types of interactions formed, where ATP interacts with several key residues involved in inhibiting receptor activity, namely Phenylalanine (PheA:1089), Asparagine (AsnA:1209), Glycine (GlyA:1087), and Proline (ProA:1158). These interactions are dominated by hydrogen bonds and hydrophobic interactions that stabilize the ligand–receptor complex in the active domain. The consistency of this interaction pattern indicates that these residues are an important part of the ATP-binding pocket and contribute to the mechanism of receptor activity inhibition, thereby reinforcing the validity of the redocking results obtained.

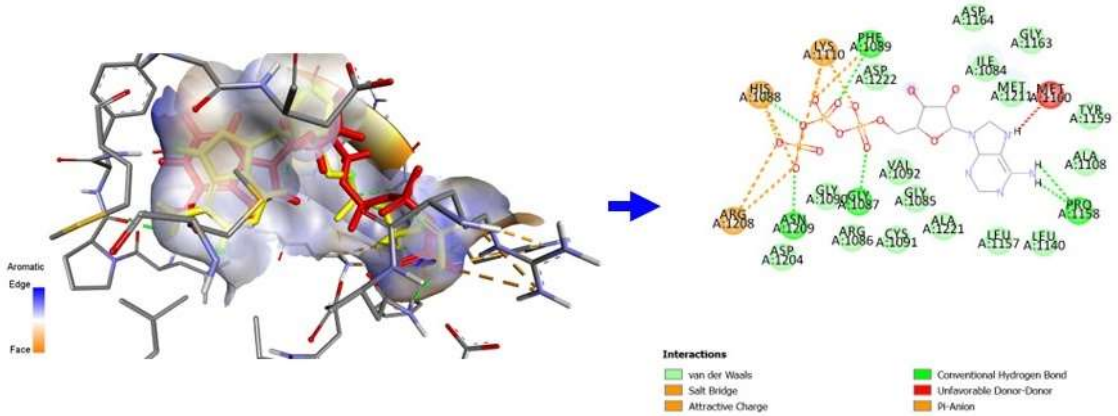

Figure 3. 3D and 2D visualization of redocking results showing consistent ligand interactions at the binding site.

Molecular Docking and Interaction Visualization

Molecular docking results indicate that several active compounds from *P.volubilis* have the potential to bind to the MET (3DKC) tyrosine kinase receptor. In Table 2, apigenin showed the best results with a ΔG value of -7.77 kcal/mol and a Ki of 2.00 µM, followed by pinoresinol with ΔG -7.57 kcal/mol, mycophenolic acid with ΔG -7.24 kcal/mol, and oleuropein aglycone with ΔG -6.90 kcal/mol. A lower ΔG value indicates that the ligand-receptor complex is more stable, while a smaller Ki value indicates better inhibitory potential. Compared to Bozitinib and ATP, Apigenin, Pinoresinol, and Mycophenolic Acid exhibited stronger binding affinities. Meanwhile, oleuropein aglycone exhibited a stronger binding affinity compared just to Bozitinib.

Table 2. Results molecular docking of ligands to receptors (3DKC).

No	Compounds	Run	Free Energy of Binding atau ΔG (kkal/mol)	Ki (µM)
1.	Reference drug (Bozitinib)	39	-6.87	9.22
2.	Native ligand (ATP)	12	-7.00	7.34
3.	Palmitoleic acid	27	-5.68	68.11
4.	Myristic acid	34	-4.87	267.47
5.	Hydroxytyrosol	48	-6.00	40.26
6.	**Pinoresinol***	61	-7.57	2.80
7.	**Apigenin***	72	-7.77	2.00
8.	**Mycophenolic acid***	23	-7.24	4.93
9.	**Oleuropein aglycone***	70	-6.90	8.76
10.	Nagilactone	10	-6.52	16.72
11.	Limonene	41	-5.83	53.68
12.	Aristolein	78	-5.74	61.98

Note: (*) indicates the best binding affinity of the selected ligand-receptor pairs for advanced analysis.

Based on the best binding results, 2D and 3D visualizations in Figure 4 demonstrate that apigenin, oleuropein aglycone, and mycophenolic acid are capable of interacting with key residues at the receptor binding site, including Asparagine (AsnA:1209), Arginine (ArgA:1208), Aspartate (AspA:1204), Methionine (MetA:1160), Glycine (GlyA:1087), and Phenylalanine (PheA:1089). The binding to the protein aligns with the native ligand-receptor interaction reference shown by the LigPlot analysis in Figure 1. Apigenin emerges as the most suitable candidate from the molecular docking stage, as it exhibits the lowest binding energy, the smallest Ki value, and an interaction pattern that supports the stability of the ligand-receptor complex.

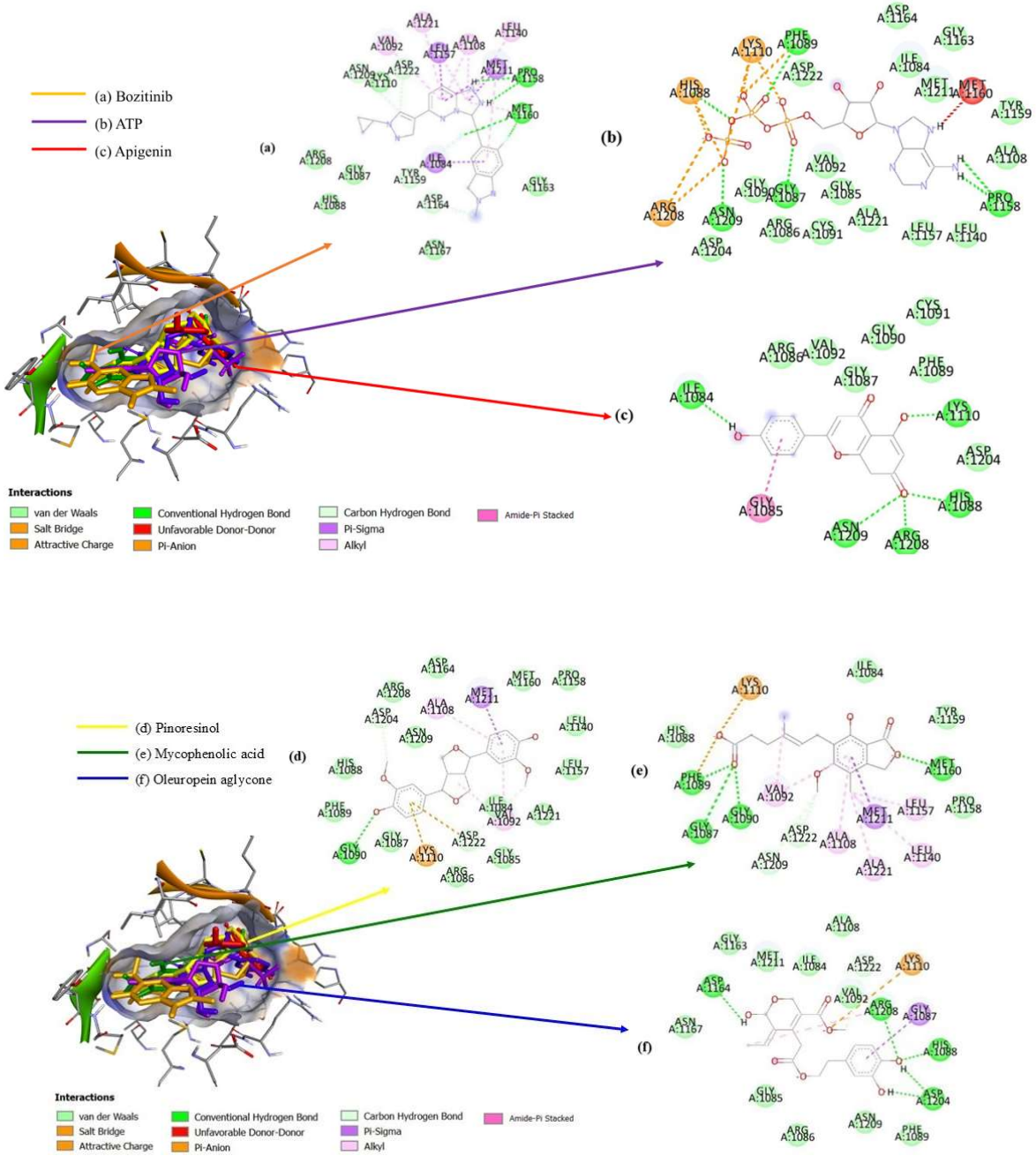

Figure 4. 3D and 2D visualizations of molecular docking results. *(a)* Reference drug (bozitinib). *(b)* Native ligand (adenosine-5′-triphosphate). *(c)* Apigenin. *(d)* Pinoresinol. *(e)* Mycophenolic acid. *(f)* Oleuropein aglycone.

Based on Figure 3, the 2D visualization of apigenin reveals the highest number of hydrogen bonds and hydrophobic interactions, and it exhibits interactions similar to those of ATP with regard to binding to the amino acids Asparagine (AsnA:1209) and Arginine (ArgA:1208). Additionally, there is an amide-π-stacked interaction, which is a weak non-covalent attraction between the amide group on the GlyA:1085 backbone and the π-electron portion of the ligand's aromatic ring, which helps stabilize the protein-ligand complex. The involvement of amide-π-stacked interactions may further support binding stability compared to standard π-stacked interactions.

According to an article by Fadhlurrohman in 2021 [22], the study, which used molecular docking methods to analyze the relatively high apigenin content in celery leaves, found that apigenin exhibits suboptimal

binding stability because its binding affinity is weaker than that of natural ligands. Apigenin does form hydrogen bonds and exhibits hydrophobic and π-stacked interactions; however, these interactions are not yet strong enough to stabilize the ligand-protein complex. Therefore, while apigenin in celery leaves holds potential as a bioactive compound, its efficacy as a breast cancer inhibitor requires further investigation.

Molecular Dynamics Simulation

Further simulations regarding the optimal binding configuration to evaluate ligand-receptor binding stability under human physiological conditions were conducted using molecular dynamics simulations. The results of these molecular dynamics simulations showed that the ligand-receptor complex exhibited varying levels of stability over the course of a 100,000 ps (100 ns) simulation. Based on the RMSD graph in Figure 5, oleuropein aglycone exhibits the best stability because it only undergoes fluctuations at the beginning of the simulation and remains stable until the end of the simulation.

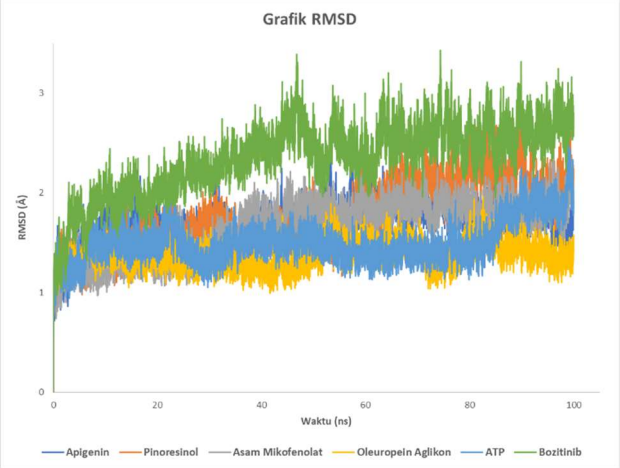

Figure 5. RMSD plots for the compounds apigenin, pinolesinol, mycophenolic acid, oleuropein aglycone, the natural ligand (ATP), and the comparator drug (bozitinib).

Figure 6 show the RMSF plot, indicating that oleuropein aglycone exhibits the lowest residue fluctuations at the binding site; therefore, the resulting complex is predicted to be more stable than other ligands, ATP, and bozitinib.

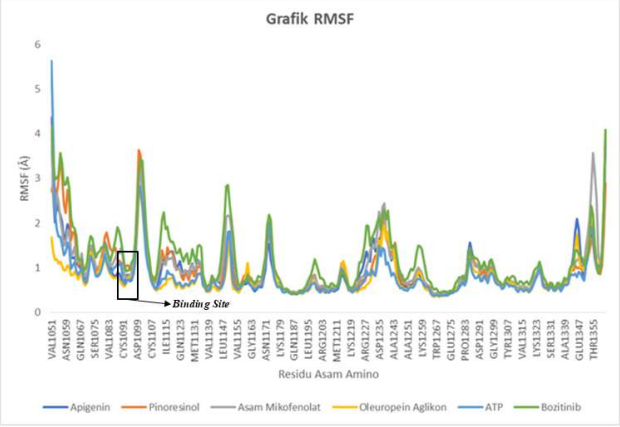

Figure 6. RMSF plots for the compounds apigenin, pinolesinol, mycophenolic acid, oleuropein aglycone, the natural ligand (ATP), and the comparator drug (bozitinib).

Based on the RMSD and RMSF plots in Figures 5 and 6, the ligand-receptor complex exhibited the highest stability, with an average RMSD value of 1.3708 Å for the oleuropein aglycone, indicating relatively minor structural conformational changes during the simulation [23]. The average RMSF value of oleuropein aglycone of 0.8121 Å also indicates that protein residue fluctuations are relatively low, suggesting that the formed

complex possesses stable flexibility [24]. Table 3 shows the differences in average RMSD and RMSF values for the test ligand complexes, ATP, and Bozitinib.

Table 3. Average RMSD and RMSF values for ligand-receptor complexes.

Complex	Reference drug (Bozitinib)	Native ligand (ATP)	Apigenin	Pinoresinol	Mycophenolic acid	Oleuropein aglycone
Average RMSD	2.3453Å	1.5042Å	1.6898Å	1.7839Å	1.6547Å	**1.3708Å***
Average RMSF	1.1945Å	0.8311Å	0.936174Å	0.9878218Å	1.0287Å	**0.8121Å***

Note: (*) showed the lowest average RMSD and RMSF compared to the other test ligands, ATP and bozitinib.

From the results of the main dynamic simulation, ligand-protein interactions were identified as shown in Table 4 below.

Table 4. Visualization results of molecular dynamic simulations of ligand-receptor interactions.

Compounds	Residue Interaction	
	Hydrogen Bond	**Hydrophobic Interaction**
Reference drug (Bozitinib)	**ProA:1158***, **MetA:1160***	TyrA:1159, HisA:1094
Native ligand (ATP)	AspA:1164, AspA:1222	ArgA:1208, AspA:1222, AsnA:1209, HisA:1088, ArgA:1086, GlyA:1090
Apigenin	PheA:1089, **ArgA:1208*, AsnA:1209***	HisA:1088, CysA:1091
Pinoresinol	AspA:1164, **MetA:1160*, LysA:1110***, GlyA:1087	AspA:1222, TyrA:1159
Mycophenolic acid	-	MetA:1211, LeuA:1140, AlaA:1221, Met:1160, ValA:1092, AlaA:1108, LeuA:1157
Oleuropein aglycone	AsnA:1209, AspA:1204	GlyA:1085, AspA:1222, PheA:1089, HisA:1088

Note: (*) showed the best ligand-receptor binding affinity and is consistent with the complex interactions resulting from the docking.

Based on the ligand-protein binding complexes in Table 3, further analysis was conducted to visualize the superimposition, as shown in Figure 7. The bozitinib, apigenin, and pinoresinol complexes exhibited good structural overlap during the 100 ns simulation. This indicates that both complexes are relatively stable and do not undergo significant conformational changes. Bozitinib and apigenin exhibited stable ligand-receptor interactions, whereas pinoresinol remained capable of maintaining interactions within the 3DKC receptor active site, primarily through residues MetA:1160 and LysA:1110. However, the ligand orientation shifted over the simulation time, meaning the ligand was not fully stable within the active pocket. Thus, apigenin has potential as a candidate c-Met inhibitor from *P.volubilis*.

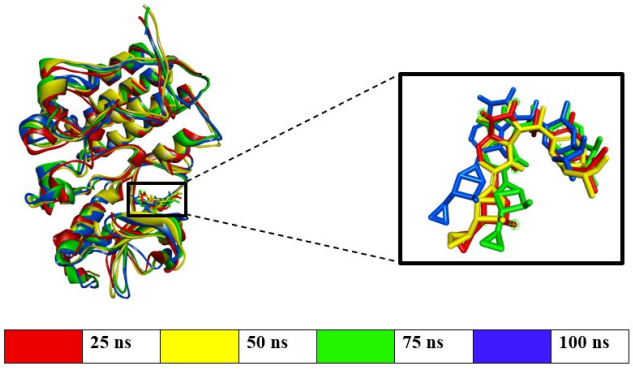

(a)

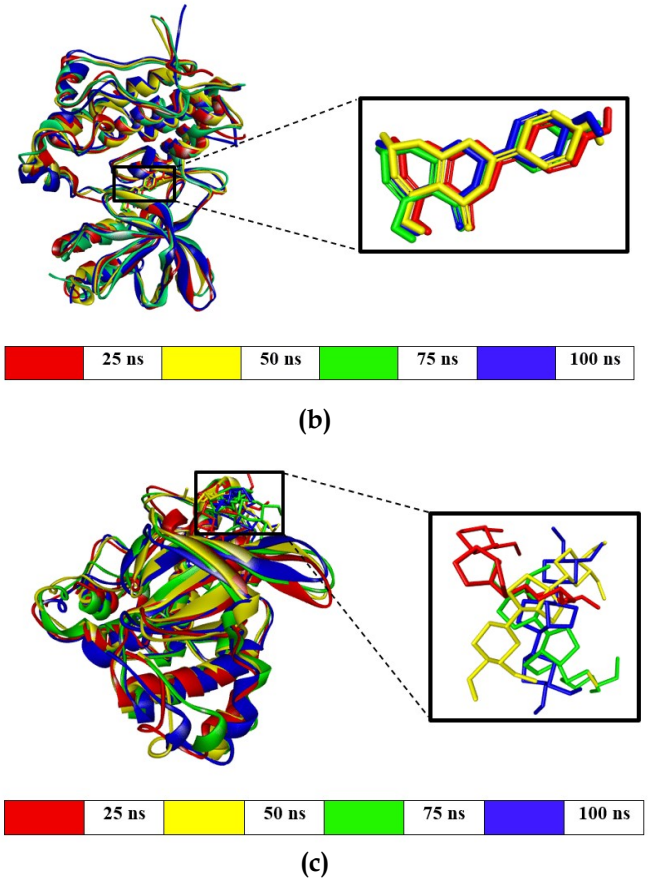

Figure 7. 3D and 2D visualizations of molecular docking results. *(a)* Reference drug (bozitinib). *(b)* Native ligand (adenosine-5′-triphosphate). *(c)* Apigenin. *(d)* Pinoresinol. *(e)* Mycophenolic acid. *(f)* Oleuropein aglycone.

The MMGBSA analysis supports the main simulation results, which were carried out for 100,000 ps [20], showing that oleuropein aglycone has a total ΔG value of −54.9309 kcal/mol, followed by apigenin with a total ΔG value of −52.8428 kcal/mol. However, the MMPBSA results indicate that apigenin exhibits the best binding free energy, with a value of approximately −24.5392 kcal/mol, compared to oleuropein aglycone and mycophenolic acid, which show similar optimal binding free energy values relative to ATP and Bozitinib, as presented in Table 5.

Table 5. Results of MMGBSA and MMPBSA analysis of the ligand–receptor complex.

Parameter	Bozitinib	ATP	Apigenin	Pinoresinol	Mycophenolic acid	Oleuropein aglycone
	Kcal/mol					
ΔGTOTAL MMGBSA	-45.9132	-50.218	**-52.8428***	-21.2530	-45.1705	**-54.9309***
ΔGTOTAL MMPBSA	-8.9890	16.8862	**-24.5392***	-1.1697	**-10.7481***	**-16.3522***

Note: (*) showing the strongest binding free energy between the ligand–receptor complex compared to other test ligands, ATP, and Bozitinib.

Therefore, oleuropein aglycone exhibits the best dynamic stability based on RMSD and RMSF analyses, whereas apigenin shows the best binding affinity based on MMPBSA results. Overall, the molecular dynamics simulation results indicate that apigenin and oleuropein aglycone are the most promising compounds in forming stable complexes with the tyrosine kinase MET receptor (3DKC).

Based on the GB/PB algorithm calculations presented in Table 4, differences between MMGBSA and MMPBSA results arise due to the distinct approaches used to estimate solvation energy. In MMGBSA, the

Generalized Born model tends to produce a more simplified estimation, resulting in more negative total ΔG values. In contrast, MMPBSA employs the Poisson–Boltzmann model, which provides a more detailed and accurate calculation of solvent electrostatic contributions [25]. This leads to a larger polar solvation penalty, resulting in higher (less negative) binding free energy values compared to MMGBSA. Thus, these differences do not indicate conflicting results, but rather reflect that the stability of the protein–ligand complex is governed by a balance of van der Waals interactions, electrostatic interactions, and solvation effects.

Pharmacokinetic Analysis

Pharmacokinetic analysis using pkCSM shows that each compound exhibits distinct ADMET profiles. Pinoresinol and apigenin demonstrate high intestinal absorption, at 93.29% and 93.25%, respectively, indicating strong potential for good oral bioavailability. Apigenin also shows favorable distribution with a VDss value of 0.822, does not inhibit CYP2D6 or CYP3A4, has a total clearance of 0.566, and is predicted to be non-hepatotoxic [21]. In contrast, pinoresinol is predicted to inhibit CYP3A4 and exhibit slower elimination, while oleuropein aglycone and nagilactone show potential hepatotoxicity. Therefore, apigenin, which exhibits the strongest binding affinity and the most stable complex formation compared to other test ligands, the native ligand (ATP), and the reference drug (Bozitinib), supported by the most optimal pharmacokinetic and toxicity profile, emerges as a promising anticancer candidate for gastric cancer derived from *Plukenetia volubilis* L.

▪ DISCUSSION

Molecular docking analysis showed that all tested compounds were able to occupy the active-site region of the c-MET receptor (PDB ID: 3DKC), including interactions with the hinge region involved in ATP recognition. This finding is consistent with previous structural studies showing that the ATP-binding site and hinge region are important recognition sites for c-MET kinase inhibitors. In particular, residues Pro1158, Tyr1159, and Met1160 in the hinge region are frequently involved in interactions with ATP-competitive c-MET inhibitors, while interactions with residues in the activation loop, such as Tyr1230, may further contribute to binding affinity and selectivity [26]. Therefore, the ability of the investigated compounds to occupy this region provides an initial indication of their potential to interact with the c-MET kinase domain. However, docking was performed using a relatively rigid receptor model and therefore primarily represents a predicted binding pose rather than the behavior of the complex under physiological conditions [26].

The molecular dynamics (MD) simulations provided additional information regarding the dynamic stability of the protein–ligand complexes. Based on the RMSD and RMSF profiles, the oleuropein aglycone–c-MET complex exhibited the greatest structural stability among the investigated complexes, as indicated by relatively low structural deviation and stable residue fluctuations throughout the simulation. The relatively stable RMSF profile in regions surrounding the active site further suggests that ligand binding did not induce substantial destabilization of the protein structure. Similar MD-based studies have used RMSD and RMSF as complementary parameters to evaluate global structural stability and local residue flexibility during protein–ligand simulations. Nevertheless, structural stability and binding affinity represent different properties and should therefore not be interpreted as equivalent measures of inhibitory activity [27].

The interaction analysis obtained from 2D snapshots further showed that interactions involving the hinge region were maintained for several complexes, including pinoresinol and the reference ligand. This observation is consistent with structural studies of c-MET inhibitors, in which hinge recognition represents a common feature of ATP-competitive binding. Previous studies have demonstrated that interactions with Pro1158 and Met1160 are characteristic of c-MET ATP-site inhibitors, while additional contacts with the activation loop, particularly Tyr1230, can contribute to ligand recognition and selectivity [26]. Thus, the observed hinge-region interactions in the present study support the relevance of this region for ligand binding, although the presence of a single interaction should not by itself be considered sufficient evidence of inhibitory activity.

Interestingly, the ranking obtained from the binding free energy calculations did not completely correspond to the RMSD and RMSF results. Apigenin exhibited the most favorable binding free energy in the MMPBSA analysis, indicating energetically favorable interactions with c-MET compared with the other investigated ligands, ATP, and the reference drug Bozitinib. This difference highlights that structural stability and binding energetics describe distinct characteristics of a protein–ligand complex. A ligand may maintain a relatively stable complex while not necessarily exhibiting the most favorable estimated binding free energy,

and conversely, a ligand with favorable energetic contributions may show greater structural fluctuations during the simulation [28]. Therefore, the favorable MMPBSA result for apigenin should be interpreted as evidence supporting its potential binding to c-MET rather than as direct evidence of biological inhibitory activity.

The differences among RMSD, RMSF, interaction snapshots, and binding free energy calculations can be explained by the different properties evaluated by each parameter. RMSD reflects changes in the overall structural conformation of the protein or complex, whereas RMSF describes residue-level flexibility. Snapshot analysis identifies specific intermolecular interactions at selected points during the trajectory, while MMGBSA and MMPBSA estimate binding free energies from multiple conformations sampled during molecular dynamics [27]. Consequently, agreement among these parameters is not necessarily expected. The use of multiple complementary approaches is therefore important for obtaining a more comprehensive interpretation of protein–ligand behavior.

The differences between docking and MD results are also attributable to the different levels of system representation. Molecular docking generally uses a simplified representation of the receptor and solvent environment to efficiently predict ligand poses. In contrast, MD simulations allow the protein, ligand, solvent molecules, and ions to undergo time-dependent movements under the selected thermodynamic conditions. This dynamic treatment can reveal conformational changes and interactions that are not captured by a single docking pose [29]. However, MD simulations remain dependent on the selected force field, simulation length, initial structure, and system preparation. In the present study, the protonation states were assigned during system preparation and were maintained throughout the conventional MD simulations; therefore, changes in protonation state during the trajectory were not explicitly modeled. This limitation should be considered when interpreting hydrogen-bonding and electrostatic interactions.

Differences in the MMGBSA and MMPBSA results may also arise from the different implicit-solvent models used to estimate the polar solvation contribution. MMGBSA employs the Generalized Born approximation, whereas MMPBSA uses the Poisson–Boltzmann approach. Both methods estimate end-point binding free energies from molecular mechanics energies and solvation contributions using snapshots obtained from MD trajectories, but their treatment of electrostatic solvation differs [28]. Consequently, differences in the magnitude and ranking of calculated binding free energies between the two methods are possible and should not be interpreted as contradictory results.

The present findings should also be considered in relation to the established structural characteristics of c-MET inhibitors. Previous structural analyses of clinically relevant c-MET inhibitors demonstrated that ATP-site inhibitors commonly anchor within the hinge region and may establish additional interactions with the activation loop, particularly Tyr1230. The interactions observed for the investigated compounds therefore provide a structural basis for their predicted association with the c-MET kinase domain. However, the present study does not establish whether these interactions translate into inhibition of c-MET kinase activity or suppression of cancer cell proliferation.

Several limitations should be acknowledged. First, the docking calculations were based on a relatively rigid receptor representation and therefore may not fully capture receptor flexibility during ligand recognition. Second, the MD simulations were performed for a finite simulation period and represent a computational approximation of the biological environment. Longer simulations and independent replicate trajectories could provide stronger evidence regarding the reproducibility and stability of the observed complexes. Third, MMGBSA and MMPBSA are end-point free energy approaches that involve approximations in the treatment of solvation and entropy and therefore should not be regarded as equivalent to experimentally determined binding free energies. In addition, the present computational analysis did not experimentally validate c-MET inhibition, cellular activity, or selectivity against other kinases. The predicted ADMET properties were also computational estimates and may differ from experimental pharmacokinetic or toxicological profiles.

Overall, the integration of molecular docking, MD simulations, and binding free energy calculations provides complementary evidence regarding the interaction, dynamic stability, and estimated binding energetics of the investigated compounds toward c-MET. Oleuropein aglycone showed the most favorable dynamic stability based on RMSD and RMSF analyses, whereas apigenin demonstrated the most favorable MMPBSA binding free energy and favorable predicted ADMET characteristics. On the whole, these findings support apigenin as a promising lead compound for further development as a potential c-MET inhibitor. Further experimental studies, including enzymatic c-MET inhibition assays, cellular assays, selectivity

evaluation, and in vivo investigations, are required to determine whether the computationally predicted interactions translate into measurable biological activity.

▪ CONCLUSION

Based on an integrated evaluation of molecular docking, molecular dynamics, MM/PBSA, and ADMET profiles, several bioactive compounds from *Plukenetia volubilis* L. demonstrated potential to interact with the c-MET tyrosine kinase receptor (PDB ID: 3DKC). Although several compounds exhibited favorable docking affinities, molecular dynamics simulations indicated differences in the stability of their interactions with the receptor. MM/PBSA analysis further identified apigenin as having the most favorable binding free energy among the evaluated compounds, while its ADMET profile showed favorable absorption, distribution, metabolism, and toxicity characteristics. In contrast, some compounds with favorable docking or binding free energy profiles showed less favorable dynamic stability or predicted toxicity. On the whole, apigenin emerged as the most promising lead compound based on the combined molecular interaction, binding free energy, dynamic stability, and ADMET assessments, supporting its potential for further development as a c-MET inhibitor candidate. Further in vitro and in vivo studies are required to validate its inhibitory activity, mechanism of action, pharmacological effects, and safety.

Acknowledgements: The authors would like to express their sincere gratitude to the Faculty of Pharmacy, Universitas Bakti Tunas Husada, for providing academic support and computational facilities necessary for this research. The authors are especially grateful to their supervisors for their valuable guidance, constructive suggestions, and continuous support throughout the study. The authors also acknowledge the Computational Laboratory of Universitas Bakti Tunas Husada for providing the facilities and resources required to conduct the molecular docking and molecular dynamics analyses.

Funding: This research received no external funding.

Conflict of interest statement: The authors declare no conflict of interest.

REFERENCES

[1] D. M. Hausman and D. M. Hausman, "What Is Cancer ?," vol. 62, no. 4, pp. 778–784, 2019, doi: doi.org/10.1353/pbm.2019.0046.

[2] C. Juni, "Kanker lambung : kenali penyebab sampai pencegahannya," vol. 3, no. 3, pp. 144–152, 2020, doi: doi.org/10.18051/JBiomedKes.2020.v3.144-152.

[3] L. Zhou, B. Han, Y. Yuan, Z. Dong, Y. Shi, and R. Zheng, "The global burden of stomach cancer and its risk factors from 1990 to 2021 : findings from the Global Burden of Disease Study 2021," 2025, doi: doi.org/10.1186/s12889-025-23901-y.

[4] H. Sung *et al.*, "Global Cancer Statistics 2020 : GLOBOCAN Estimates of Incidence and Mortality Worldwide for 36 Cancers in 185 Countries," vol. 71, no. 3, pp. 209–249, 2021, doi: 10.3322/caac.21660.

[5] M. C. S. Wong, J. Huang, P. S. F. Chan, P. Choi, X. Q. Lao, and S. M. Chan, "Global Incidence and Mortality of Gastric Cancer , 1980-2018," vol. 4, no. 7, pp. 1–14, JAMA Network Open, 2021, doi: 10.1001/jamanetworkopen.2021.18457.

[6] Y. Zhang, L. Shen, and Z. Peng, "Advances in MET tyrosine kinase inhibitors in gastric cancer," vol.21, no.6, Cancer Biol Med, 2024, doi: 10.20892/j.issn.2095-3941.2024.0044.

[7] M. Zhao, F. Wei, G. Sun, Y. Wen, and J. Zeng, "Natural compounds targeting glycolysis as promising therapeutics for gastric cancer : A review," no. November, pp. 1–21, 2022, doi: 10.3389/fphar.2022.1004383.

[8] F. Ramos-Escudero, M. T. Morales, M. Ramos Escudero, A. M. Muñoz, K. Cancino Chavez, and A. G. Asuero, "Assessment of phenolic and volatile compounds of commercial Sacha inchi oils and sensory evaluation," *Food Res. Int.*, vol. 140, p. 110022, 2021, doi: 10.1016/j.foodres.2020.110022.

[9] N. Apriana, Riska, N. Bialangi, L. Alio, Y. K. Salimi, L. Ode Aman, and A. Kadir Kilo, "Identifikasi senyawa

metabolit sekunder dan analisis total fenolik ekstrak metanol daun sacha inchi (Plukenetia volubilis linneo) yang tumbuh di Gorontalo," *J. Pendidikan, Kim. Fis. dan Biol.*, vol. 1, no. 3, pp. 193–207, 2025.

[10] N. A. R. Mhd Rodzi and L. K. Lee, *Sacha Inchi (Plukenetia Volubilis L.): recent insight on phytochemistry, pharmacology, organoleptic, safety and toxicity perspectives*, vol. 8, no. 9. Elsevier Ltd, 2022. doi: 10.1016/j.heliyon.2022.e10572.

[11] N. Anis, R. Mhd, and L. K. Lee, *Sacha Inchi (Plukenetia Volubilis L.): recent insight on phytochemistry, pharmacology, organoleptic, safety and toxicity perspectives*. Elsevier Ltd, 2022. doi: 10.1016/j.heliyon.2022.e10572.

[12] A. Parvaiz, "Synergistic Action of Tlp and Pr1 Proteins Revealed Their Enhanced Interaction With Fungal Cell-Wall Components: Evidence From in Silico Studies," *Agrobiol. Rec.*, vol. 22, pp. 129–140, 2025, doi: 10.47278/journal.abr/2025.055.

[13] R. Ruswanto, T. No, R. Mardianingrum, and D. Kesuma, "Heliyon Design , molecular docking , and molecular dynamics of thiourea-iron (III) metal complexes as NUDT5 inhibitors for breast cancer treatment," vol. 8, no. July, Heliyon, 2022, doi: 10.1016/j.heliyon.2022.e10694.

[14] D. Atsna, N. Salsabila, T. Herlina, and D. Kurnia, "Antimicrobial Activities of Crocatin B From Piper crocatum as an Antithroat Infection : In Vitro and In Silico Studies," pp. 1–13, Journal of Chemistry, 2026, doi: 10.1155/joch/5292752.

[15] A. T. McNutt, F. Bisiriyu, S. Song, A. Vyas, G. R. Hutchison, and D. R. Koes, "Conformer Generation for Structure-Based Drug Design: How Many and How Good?," *J. Chem. Inf. Model.*, vol. 63, no. 21, pp. 6598–6607, Journal of Chemical Information and Modeling, 2023, doi: 10.1021/acs.jcim.3c01245.

[16] M. E. Effiong, M. Bella-Omunagbe, I. S. Afolabi, and S. N. Chinedu, "Molecular Docking Appraisal of Pleurotus ostreatus Phytochemicals as Potential Inhibitors of PI3K/Akt Pathway for Breast Cancer Treatment," *Bioinform. Biol. Insights*, vol. 19, 2025, doi: 10.1177/11779322251316864.

[17] S. Kumar *et al.*, "Discovery of New Hydroxyethylamine Analogs against 3CL pro Protein Target of SARS-CoV-2 : Molecular Docking , Molecular Dynamics Simulation , and Structure − Activity Relationship Studies," 2020, doi: 10.1021/acs.jcim.0c00326.

[18] M. R. Fadhil Pratama, H. Poerwono, and S. Siswodihardjo, "Introducing a two-dimensional graph of docking score difference vs. similarity of ligand-receptor interactions," *Indones. J. Biotechnol.*, vol. 26, no. 1, pp. 54–60, 2021, doi: 10.22146/IJBIOTECH.62194.

[19] M. Manish, S. Mishra, A. Anand, and N. Subbarao, "Computational molecular interaction between SARS-CoV-2 main protease and theaflavin digallate using free energy perturbation and molecular dynamics," *Comput. Biol. Med.*, vol. 63, no. 21, pp. 6698-6607, Journal of Chemical Information and Modeling, 2022, doi: 10.1016/j.compbiomed.2022.106125.

[20] C. G. Yang, T. Chen, W. T. Si, A. H. Wang, H. C. Ren, and L. Wang, "High-performance PBPK model for predicting CYP3A4 induction-mediated drug interactions: a refined and validated approach," *Front. Pharmacol.*, vol. 16, February, pp. 1–12, 2025, doi: 10.3389/fphar.2025.1521068.

[21] I. U. Khan, A. Singh, S. Singh, and B. P. S. Sagar, "Drug Induced Hepatotoxicity and Hepatoprotective Drugs : A Review," vol. 8, no. 9, pp. 351–375, 2023.

[22] D. Fadhlurrohman and Ruswanto, "Study In Silico Senyawa Apigenin Saledri (Avium graveolens) Sebagai Antikanker Terhadap Kanker Payudara," pp. 1–7, 2021.

[23] Kuschner, O'connor, and A. M. Butz, "Aromatic interactions at the ligand-protein interface: Implications for the development of docking scoring functions," *Physiol. Behav.*, vol. 176, no. 12, pp. 139–148, 2017, doi: 10.1111/cbdd.13084.Aromatic.

[24] R. Mardianingrum, S. R. N. Endah, E. Suhardiana, R. Ruswanto, and S. Siswandono, "Docking and molecular dynamic study of isoniazid derivatives as anti-tuberculosis drug candidate," *Chem. Data Collect.*, vol. 32, p. 100647, 2021, doi: 10.1016/j.cdc.2021.100647.

[25] F. Zare *et al.*, "A combination of virtual screening, molecular dynamics simulation, MM/PBSA, ADMET, and DFT calculations to identify a potential DPP4 inhibitor," *Sci. Rep.*, vol. 14, no. 1, pp. 1–16, 2024, doi: 10.1038/s41598-024-58485-x.

[26] I. C. Russell *et al.*, "Molecular Basis of c-MET Inhibition by Approved Small Molecule Drugs: A Structural Perspective," *ACS Med. Chem. Lett.*, vol. 17, no. 3, pp. 590–597, 2026, doi: 10.1021/acsmedchemlett.5c00713.

[27] N. Wu, R. Zhang, X. Peng, L. Fang, K. Chen, and J. S. Jestilä, "Elucidation of protein-ligand interactions by multiple trajectory analysis methods," *Phys. Chem. Chem. Phys.*, vol. 26, no. 8, pp. 6903–6915, 2024, doi: 10.1039/d3cp03492e.

[28] S. Genheden and U. Ryde, "The MM/PBSA and MM/GBSA methods to estimate ligand-binding affinities," *Expert Opin. Drug Discov.*, vol. 10, no. 5, pp. 449–461, 2015, doi: 10.1517/17460441.2015.1032936.

[29] S. R. Zia, A. Coricello, and G. Bottegoni, "Increased throughput in methods for simulating protein ligand binding and unbinding," *Curr. Opin. Struct. Biol.*, vol. 87, no. 102871, 2024, doi: 10.1016/j.sbi.2024.102871.